Iranian Journal of Materials Forming 10 (4) (2023) 52-64

Online ISSN: 2383-0042

IJMF

Iranian Journal of Materials Forming

Journal Homepage: http://ijmf.shirazu.ac.ir

Research Article

Machinability Evaluation of Al 3003 Processed by Non-Equal-Channel Angular Pressing (NECAP) Using Taguchi Method

M.H. Gholami, M. Honarpisheh* and S. Amini

Faculty of Mechanical Engineering, University of Kashan, Kashan, Iran

ARTICLE INFO

Article history:

Received 22 November 2023
Reviewed 28 February 2024
Revised 13 March 2024
Accepted 06 April 2024

Keywords:

NECAP
Machinability
Cutting force
Surface roughness
Chip formation

Please cite this article as:

Gholami, M.H., Honarpisheh, M., & Amini, S. (2023). Machinability evaluation of Al 3003 processed by non-equal-channel angular pressing (NECAP) using Taguchi method *Iranian Journal of Materials Forming*, *10*(4), 52-64.https://doi.org/10.22099/IJMF.2024.48909.1276

ABSTRACT

Non-equal-channel angular pressing (NECAP) is emerging as one of the most developed severe plastic deformations (SPD) methods that require more detailed investigations. Machining study is inevitable to form any material into required dimensions. The lack of NECAP processed materials machining data, as a fundamental stage for production development, motivated the present work, in which the machinability aspects of Al 3003 subjected to NECAP process, in terms of cutting force, surface roughness, and chip morphology have been investigated and compared to initial state of mentioned material. Experimental runs have been conducted using defined machining parameters under the name of spindle speed, feed rate, and depth of cut. The results show noticeable enhancements in which impact of NECAP process on the machinability of Al 3003 causes reducing the cutting force (10.24%), surface roughness (8.47%), and chip formation improvement. High spindle speed (1500 rev/min), low feed rate (98 mm/min), and depth of cut (0.5 mm) have been the best cutting parameters combination to achieve desired machinability aspects in both workpiece, before and after NECAP process. The paper's findings advocate the application of NECAP processed Al 3003 in manufacturing industries.

1. Introduction

Machining and machinability have received serious and meticulous attention in past years due to their indispensable role in manufacturing industries. Various processes are used to produce many industrial products, but they often need further machining for practical use. To obtain precise, reliable, safe, and cost-effective product, machinability study is inevitable. Since different materials with various microstructures and mechanical properties exhibit different machining properties, machinability investigation of new materials or those modified materials processed to improve their properties, has been a primary stage of production of these materials. On the other hand, severe plastic

* Corresponding author
E-mail address: honarpishe@kashanu.ac.ir (M. Honarpisheh)
https://doi.org/10.22099/IJMF.2024.48909.1276

deformation (SPD) methods, in particular non-equal-channel angular pressing (NECAP) as developing process to obtain modified material with outstanding properties, are requiring more detailed machinability investigations for practical application and commercialization [1].

SPD, in recent years, has gained significant recognition as one of the most rapidly evolving fields, captivating researchers' interest. Its potential to produce bulk nanostructured and ultrafine-grained forms of different materials have been the center of attention. The enhanced physical and mechanical properties inherent to ultrafine grained materials such as high strength, good ductility, superior super-plasticity, low friction coefficient, high wear resistance, enhanced high cycle fatigue life, and good corrosion resistance have been considered as advantages that lead to its increasing development [1-3]. The publication of articles on ultrafine-grained (UFG) materials highlights the growing significance of SPD annually [4-6]. The recent developments in research on UFG materials and their outstanding properties have accentuated the interest in SPD on common engineering metals [7].

Of these processes, equal-channel angular pressing (ECAP) has been prominently studied among the SPD processes [1-3, 8]. The ECAP die contains two equal cross-section channels with predefined intersecting angles. The desired sample is placed in the inlet channel and pushed through the die with the plunger. A sample with refined grains and enhanced mechanical properties comes out from the outlet channel without any change in its dimension. Like other processes, some disadvantages could be named for ECAP process that cannot be ignored. It involves the repetition of the process to achieve the required strains. It is concluded that ECAP can be successfully done in laboratory scale, but before it can be used in industrial manufacturing it must overcome a number of obstacles [9]. To avoid these limitations, non-equal-channel angular pressing (NECAP), as one of the SPD processes and modified version of ECAP process, has been considered by the researchers to obtain the remarkable strain without the need of repeating the process [10-18]. However, more or less, inherent back pressure caused due to the reduced cross section of the output channel, uniform microstructure, induced considerable strains, texture improvement and capability of implementation for industrial and manufacturing applications have also been considered as the eminence of NECAP in comparison to ECAP [11, 12, 14, 17].

Machining and machinability have a huge impact on the price of the product, and it is essential to study how easily a certain material can be economically machined. Many factors affect machinability, and it is not a unique material property that can be clearly defined and measured. There are a few different criterias of machinability that generally take into consideration several aspects of machinability separately [19-21]. Improvements in machinability are characterized by studying one or several of the items that are presented in Fig. 1.

Good machinability is related to the removal of material with minimum cutting forces, high material removal rate, good surface finish, easier chip removal, and minimum tool wear [22]. It is difficult to maintain all these objectives at once in a machining operation. Therefore, it is always a challenge for researchers to find ways to improve machinability without spoiling the desired performance. A wide variety of research has been conducted each year to study the effects of machining input parameters on machinability criteria in different materials [23-26].

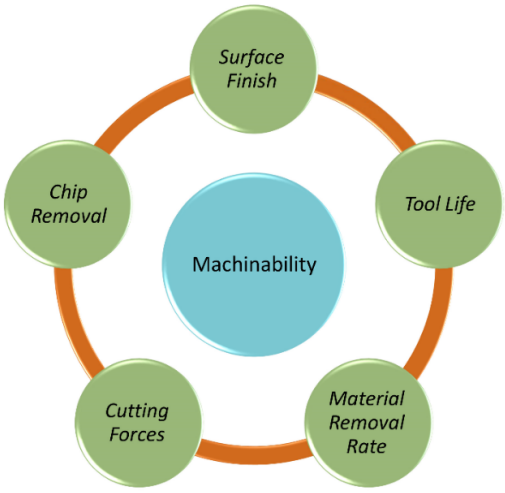

Fig. 1. Several aspects of machinability.

Of all metals, aluminum is one of the most widely used materials with properties that make it suitable for many general-purpose uses such as marine, aerospace, home appliance, motor vehicle applications etc. Due to the wide use of this metal, a lot of research has been done on its machinability [27, 28]. Sukumar et al. [29] have used Taguchi and ANN approach to study optimal machining parameters in face milling. Al-6061 has been used as a material and it has been shown that speed has the most influence on the surface finish of the part. The importance of the effect of micro-structured milling cutter on machining performance has been investigated during aluminum alloy machining by Pan et al. [30]. Selecting two types of tools, assessment of the surface quality and milling load of the machined workpiece has been considered. It has been demonstrated that microstructures reduce tool wear and enhance milling stability.

The machinability and parametric optimization of end milling on aluminum hybrid composites have been studied by Rajeswari et al. [19]. In this research, design of experiments (DOE) has been used to conduct the experimental nonlinear regression models have been developed to predict the objective function. Multi-objective genetic algorithm has been used to provide the best possible settings for the parameters. Mahanta et al. [31] have assessed the effect of the dispersing phase of SiC on the machining behavior of Al6063-SiC composite. It was found that cutting forces and hardness of the composite increased with the increase of SiC content. Sreejith [32] has studied the effect of different lubricant conditions on the machining of 6061 aluminum alloy. The influence of dry machining, minimum quantity of lubricant (MQL), and flooded coolant conditions on cutting forces, surface roughness of the machined workpiece, and tool wear have been investigated. It was observed that cutting forces were dependent on the coolant system. Rahmati et al. [33] has introduced a nanolubricant containing MoS2 nanoparticles to improve the surface morphology of the machined workpiece in the end milling of Al 6061-T6 alloy. It was reported that applying nano lubricant produced fine machined surfaces and enhanced surface quality.

Machinability of the aluminum 3003 alloy during conventional turning (CT) and Laser Assisted Turning (LAT) has been carried out by Deswal et al. [34]. It was observed that the cutting forces and discontinuous and thick chips were increased at high laser power. Surface roughness was also appeared to be higher in LAT than in CT. Yang et al. [35] have optimized energy consumption, processing time, and surface roughness of Al 3003 during the milling process using a proposed integrated framework.

As mentioned previously, SPD and machinability are two important issues that are currently being considered as research topics. However, research related to the combination of these two fields has been less reported and mainly limited to equal-channel angular pressing (ECAP) [36-38] and hydrostatic extrusion (HE) [39]. To the best of the authors' knowledge, since machinability evaluation of parts produced by SPD processes in particular NECAP process has not yet received its due attention in the research community despite years of study on this topic and it has not yet been investigated in detail, the purpose of the present paper is to provide a clear understanding of the machinability of Al 3003 subjected to the NECAP process. Based on the limitations of previous research results, the correlation between input and output machining parameters is examined as one of the essential aspects of production development. The focus is on the unique characteristics and challenges associated with machining NECAP-produced workpieces in comparison to initial workpieces. The relationship between the machinability of NECAP-produced workpieces and their microstructure and mechanical properties is explored, providing insights into the optimal machining conditions for better machinability. Additionally, the evaluation of cutting forces, surface roughness, and chip formation is discussed and highlighted, which can help in identifying potential applications of the NECAP process in various industries.

2. Experimental Procedure

2.1. Die design and workpiece preparation

NECAP consist of two intersecting channels with non-equal cross sections that are connected with a determined angle. Since the dimension of the outlet channel is smaller than inlet channel, the sample can extrude just once and large strain is attained in just one pass [15]. Schematic of the NECAP process is demonstrated in Fig. 2(a). To conduct the NECAP process, the die was designed according to the required workpiece and then manufactured. The die was composed of two different channels, which were perpendicular to each other. The input channel dimension ($20 \times 20\,mm$), the output channel dimension ($20 \times 15\,mm$), inner corner radius ($r = 4\,mm$), outer corner radius ($R = 0\,mm$) and an inner corner angel ($\phi = 90^{\circ}$) are demonstrated in Fig. 2(b). A $200\,kN$ pressing machine was used to perform the experiments. In the NECAP process, the tests were done at ambient temperatures, the ram speed was 3 mm/min and workpieces were covered by Teflon layers as lubricant.

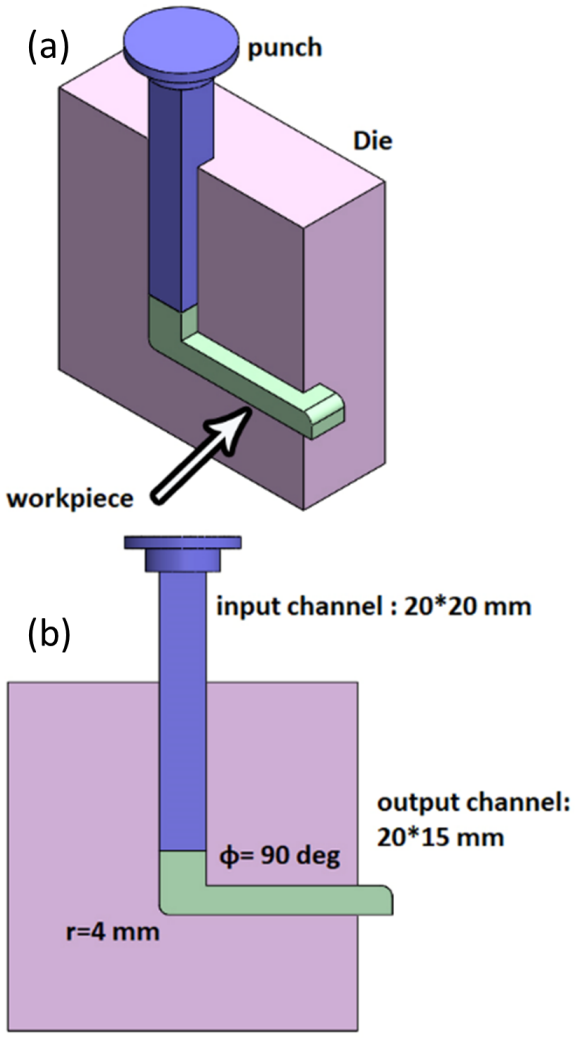

Fig. 2. (a) Schematic of NECAP process and (b) design parameters of NECAP die.

Due to the inherent adhesion property of aluminum machining, and its tendency to stick to and built-up on the tool's working tip, which affects the machinability aspects such as surface quality and cutting force, it seems, that investigating aluminum as a working material could be helpful. Thus, billets with dimensions of $70 \times 20 \times 20\,mm$ of commercial Al 3003 were used as material and its chemical composition is given in Table 1.

The billets were annealed under the temperature of 413 °C for 4 h. They were then allowed to cool in the furnace. In this paper, the annealed sample before NECAP process is called the primary workpiece and the formed workpiece after the NECAP process is called the NECAPed workpiece. Manufactured die and both workpieces are illustrated in Figs. 3(a) and 3(b).

Table 1. Chemical composition of Al 3003

Element	Fe	Cu	Si	Mn	Zn	Al
wt. %	0.70	0.05	0.60	1.5	0.10	Bal.

2.2. Machine tool and measuring equipment

The machining tests were made using Lunan zxx6350za milling machine. HSS end mill tool with diameter of 20 mm is used in machining operation. Fig. 4(a) illustrates workpiece, tool and dynamometer used in the experiments. KISTLER dynamometer model 9257B with 3.5 kHz natural frequency was employed to measure the cutting forces, installed under the workpiece. Surface roughness was measured by TR 100 equipment. Moreover, a view measuring machine (VMM) and Scanning Electron Microscopy (SEM) were utilized to analyze, surface topography and chip formation of the machined specimens. Hardness was measured using Koopa UV1 machine and tensile tests were carried out at room temperature with the strain rate of 10^{-3} s^{-1} using Santam stm/150 machine according to

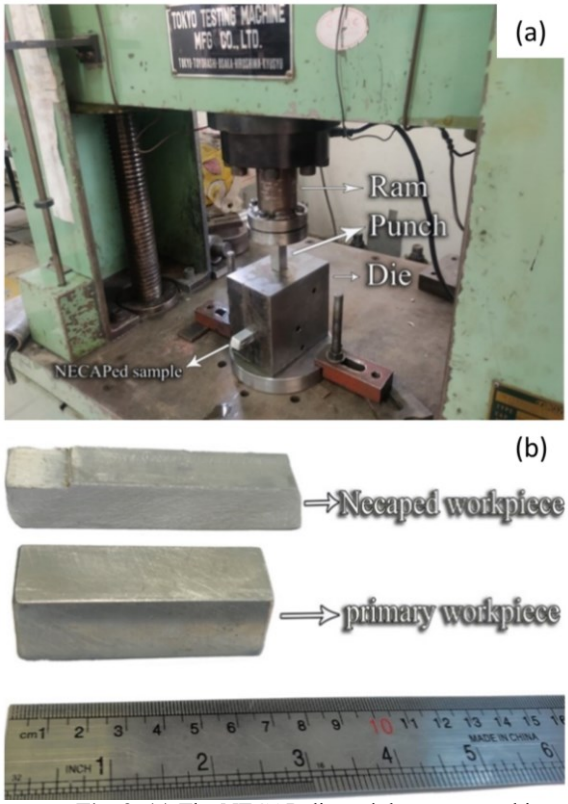

Fig. 3. (a) The NECAP die and the press machine (b) primary and the NECAPed workpieces.

ASTM E8-E8M procedure. Fig. 4(b) demonstrates equipment used for measuring surface quality.

2.3. Experimental setup and procedure

In the present work, three important machining parameters namely spindle speed, feed rate, and depth of cut were selected for analyzing the machining performance process. The levels and a typical range of machining parameters used in the machinability tests are presented in Table 2.

All machinability tests were done in dry machining conditions. According to machining parameters and their levels, L27 orthogonal array of Taguchi method was utilized to investigate any nonlinear effects of machining parameters on the machinability output to obtain a reliable result.

3. Results and Discussion

To evaluate the influence of the NECAP process on the machinability of Al 3003, milling experiments were performed on both primary and NECAPed workpieces. Table 3 shows the experimental layout and corresponding average test results for both primary and NECAPed workpieces.

3.1. Mechanical properties

According to ASTM E8-E8M procedure, small-size specimens proportional to standard for both primary and NECAPed workpiece were machined. Hardness and tensile tests were performed to compare their strength and ductility. An average of at least three measurements were reported for both hardness and tensile tests. Engineering stress-strain curves obtained from the tensile test for both samples are illustrated in Fig. 5. Comparison values of the yield strength (σ_Y), ultimate tensile strength (σ_U), fracture strain (ε_f) and toughness (T) with their changes value (CH.V.) are also presented in Fig. 6. Clearly, after NECAP process, yield strength (38.18%) and UTS value (49.08%) increase and fracture strain (47.56%), and toughness (40.55%) decrease. Since

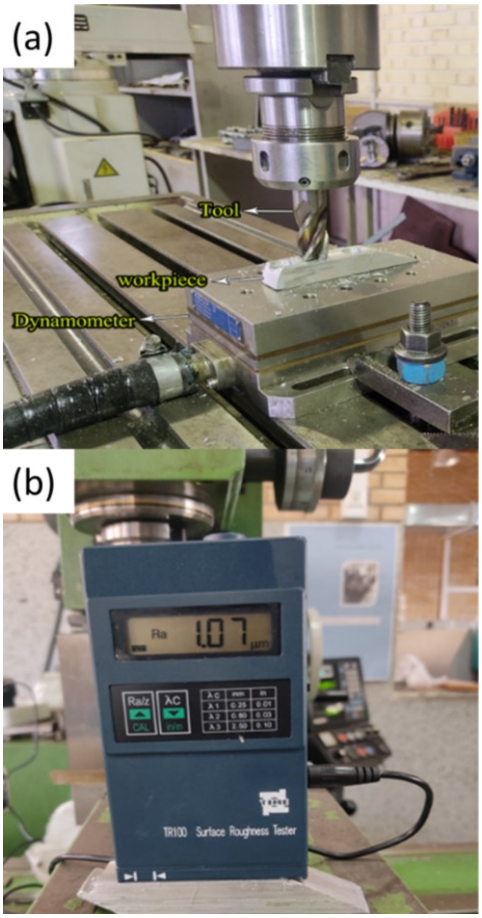

Fig. 4. (a) Milling machine, tool, and dynamometer and (b) TR100 surface roughness tester.

Table 2. Machining parameters and their levels

Control Parameters	Symbol	Unit	Level 1	Level 2	Level 3
Spindle speed	n	rev/min	565	950	1500
Feed rate	f	mm/min	98	132	200
Depth of cut	a_p	mm	0.5	1	1.5

toughness is defined as the energy absorbed by the material before the fracture and it is equivalent to the area under the stress–strain curve, therefore, the ductility of the material decreases after NECAP process. It is also clear from Fig. 6 that hardness values increased from 25.38 HV for the primary specimen to 50.34 HV for the NECAPed specimen after NECAP process. Based on the following equation [10, 16], equivalent plastic strain of this process is equal to 1.2009.

$$\varepsilon = (\frac{P}{C} + \frac{C}{P})/\sqrt{3} \quad (1)$$

Where P is the input channel thickness, and C is the output channel thickness. (P=20 mm, C=15 mm in the present study)

Table 3. Experimental results

Experimental run	Machining parameters			Measured outputs of primary workpiece		Measured outputs of NECAPed workpiece	
	Spindle speed (rev/min)	**Feed rate (mm/min)**	**Depth of cut (mm)**	**F_R (N)**	**R_a (μm)**	**F_R (N)**	**R_a (μm)**
1	1	1	1	44.75	0.62	40.10	0.59
2	1	1	2	60.39	0.66	55.06	0.64
3	1	1	3	86.04	0.71	80.20	0.69
4	1	2	1	50.16	0.79	45.19	0.76
5	1	2	2	64.68	0.95	58.27	0.86
6	1	2	3	89.23	1.2	80.39	0.99
7	1	3	1	62.48	1.25	59.08	1.12
8	1	3	2	82.25	1.82	78.24	1.68
9	1	3	3	116.74	2.3	110.14	2.05
10	2	1	1	39.25	0.55	35.12	0.52
11	2	1	2	54.34	0.62	50.21	0.59
12	2	1	3	70.54	0.7	65.07	0.65
13	2	2	1	36.51	0.76	32.89	0.73
14	2	2	2	58.05	0.85	52.3	0.8
15	2	2	3	72.86	1.15	65.64	0.96
16	2	3	1	45.07	1.11	40.12	1.02
17	2	3	2	69.91	1.61	65.17	1.53
18	2	3	3	86.23	1.94	80.27	1.84
19	3	1	1	30.91	0.48	25.13	0.45
20	3	1	2	47.04	0.55	43.22	0.52
21	3	1	3	63.30	0.62	58.31	0.57
22	3	2	1	33.40	0.65	28.12	0.63
23	3	2	2	48.93	0.76	45.36	0.7
24	3	2	3	65.00	0.98	59.24	0.82
25	3	3	1	38.81	0.99	34.96	0.91
26	3	3	2	60.93	1.43	54.89	1.36
27	3	3	3	78.90	1.88	71.09	1.63

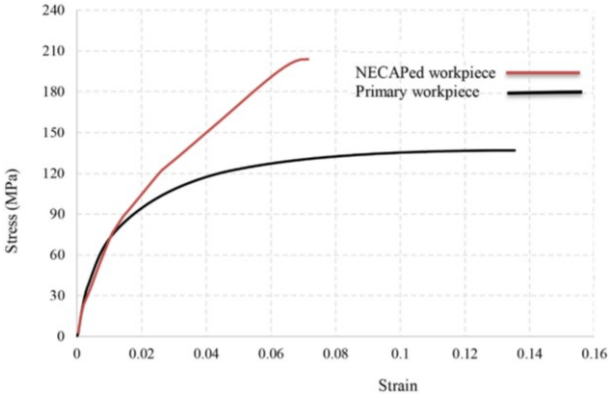

Fig. 5. Engineering stress–strain curves.

The considerable strength and hardness improvement in the NECAP process can be attributed to the severe reduction of the grain size and grain refinement. In summary, the NECAP process leads to grain refinement, resulting in an enhancement in yield strength and ultimate tensile strength, as well as a decrease in fracture strain and ductility.

3.2. Cutting force analysis

While milling, cutting forces are exerted in three planes to deform and shear away material in the form of a chip. The components of cutting forces in three directions are tangential (F_x or F_t), radial or normal (F_y *or* F_r), and axial force (F_z) that were measured using a mentioned dynamometer connected to PC. The cutting forces of all cutting conditions have been studied for their similarities and differences. Since a similar trend for cutting forces components in three directions (F_x, F_y, and F_z) is observed, thus using Eq. (2) [40], the resultant cutting force for each experiment is calculated according to the relevant average of each measured component shown in Table 3.

$$F_R = \sqrt{F_x^2 + F_y^2 + F_z^2} \qquad (2)$$

Fig. 7 is representative of all combinations and shows what happens to cutting forces by varying spindle speed at different depths of cuts and feed rates for both primary and NECAPed workpieces. While the spindle speed increases, cutting forces decrease in all cutting conditions. The reason behind this is that as spindle speed increases, heat generation in the cutting zone also increases, leading to a softening effect and a reduction in cutting force. In other words, by increasing the spindle speed, the temperature in the flow zone rises, and the shear strength drops.

Apart from spindle speed variation, it is observed that the cutting forces increase with feed increment at a stable depth of cut. This is due to the fact that as the feed increases, chip load per tooth increases, and workpiece resistance against shear maximizes [41]. As a result, the required force for machining increases. In addition, as can be seen in Fig. 7, by increasing the depth of cut under a constant feed rate, the cutting force increases. It could be described by the fact that increasing the depth of cut has led to an increase in the effective area of shear per tooth. This, in turn, results in an increment in chip volume and deformed chip thickness. As a result, the cutting force increases accordingly. As Fig. 7 demonstrates, the cutting force value of the primary specimen is higher than the NECAPed specimen (average 10.24%), while the primary specimen has higher mechanical properties, such as yield stress, ultimate tensile strength (UTS), and hardness. This phenomenon is attributed to two issues: first, cold work on materials decreases frictional forces between the cutting tool edge and chip, thus requiring lower cutting forces for machining the NECAPed specimen. Second, lower ductility and improvements in hardness and ultimate tensile strength (UTS) result in a decrease in material adhesion [37]. As aluminum is an adhesive material, a built-up layer (BUL) was formed on the cutting edge of the tool during the machining of the primary workpiece as shown in Fig. 8. In fact, the low

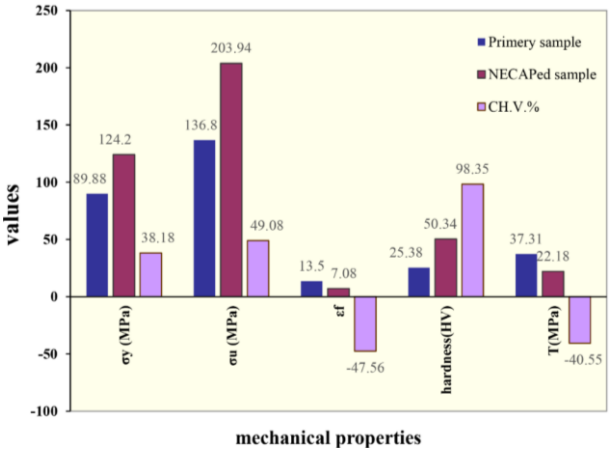

Fig. 6. Comparison of the mechanical properties of both specimens.

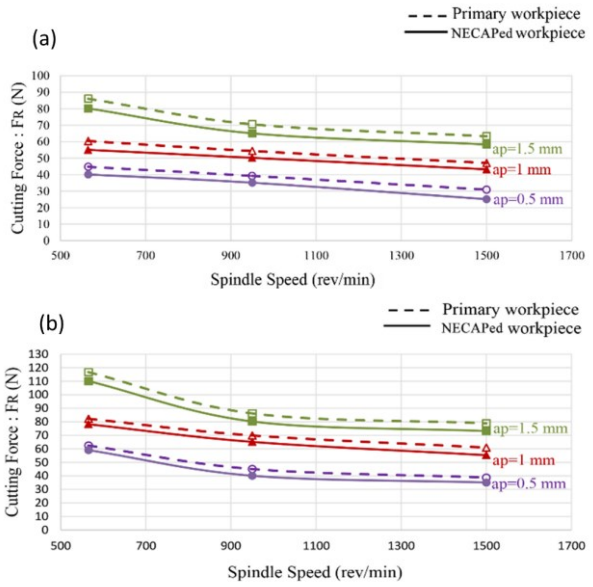

Fig. 7. Effect of spindle speed on a cutting force for both workpieces: (a) feed: 98 mm/min and (b) feed: 200 mm/min.

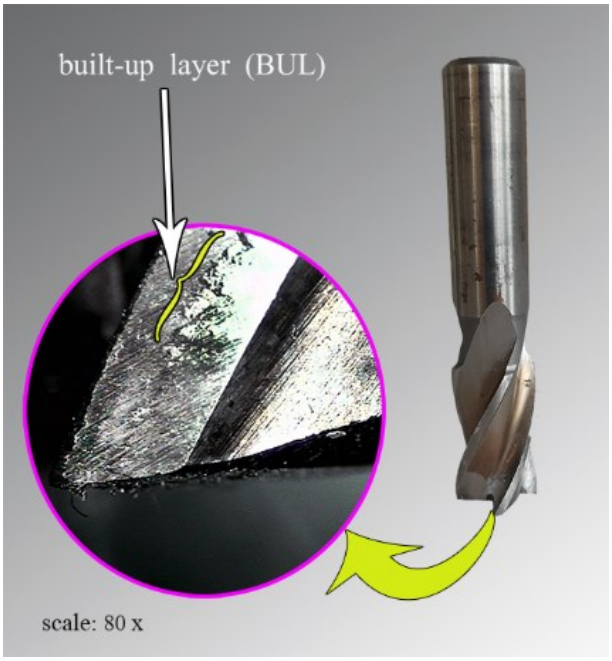

Fig. 8. A built-up layer (BUL) on the tool face.

hardness and high ductility of the primary workpiece, in comparison to the NECAPed workpiece (section 3.1), provide a higher possibility of BUL formation on a tool tip, which in turn, increases cutting forces. This phenomenon is due to the fact that as the hardness of the material decreases, adhesion of materials to the cutting tool increases, which in turn leads to BUL formation.

3.3. Surface roughness analysis

The sampling area was randomly selected at various positions of workpiece surfaces, and surface roughness was measured in the feed direction for each machining condition. To obtain reliable results, the average of surface roughness values measured at three sampling areas is considered for the analysis. An experimental measured data for surface roughness is illustrated in Table 3. Fig. 9 is representative of all combinations and depicts what happens to surface roughness by cutting speed during various rates of feed and depth of cut for both workpieces.

It is obvious that by maximizing the spindle speed, minimizing the surface roughness occurs. High spindle speed leads to a simpler and easier deformation process, which can be attributed to generating higher temperature. It is also clear that surface roughness increases with increasing feed rate and depth of cut for both workpieces. Clearly, the lower surface roughness was observed in NECAPed workpiece. As mentioned earlier, both workpieces were machined under the same cutting conditions. Thus, it could be concluded that differences in surface roughness are related to material properties and structure. An enhancement in the strength and hardness, and a loss of ductility of the NECAPed specimen, have facilitated the chip flow on the cutting tool. This leads to a reduction of chip adhesion on the tool face and, as a result, improves the surface finish of the NECAPed part. In addition, grain refinement is reducing the resistance forces between the workpiece and tool, thereby decreasing the cutting temperature. This, in turn, increases the surface finish of the NECAPed part. The brittle and harder nature of the NECAPed workpiece plays a significant role in the interaction between the cutting tool and the workpiece surface, which results in a better surface finish. As shown in Fig. 10, the presence of piled-up aluminum particles on the tool face during the machining of the primary workpiece results in higher surface roughness compared to the NECAPed workpiece. In addition, as mentioned previously, the material adhesion decrement of the NECAPed workpiece prevents BUL formation,

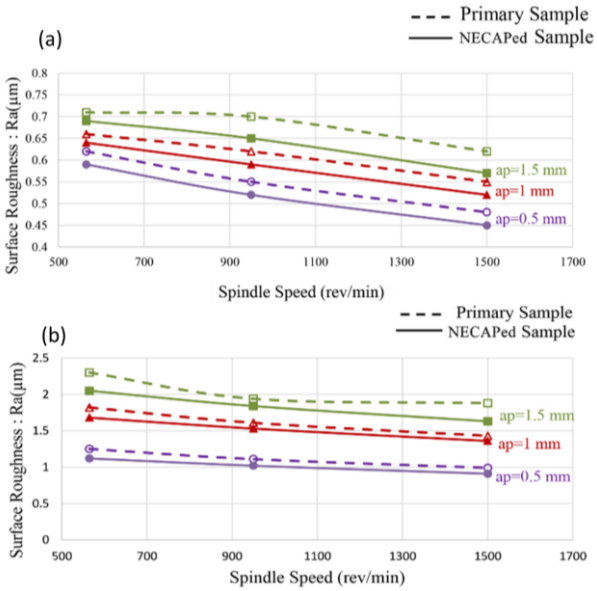

Fig. 9. Effect of spindle speed on a surface roughness for both workpieces (a) feed: 98 mm/min and (b) feed: 200 mm/min.

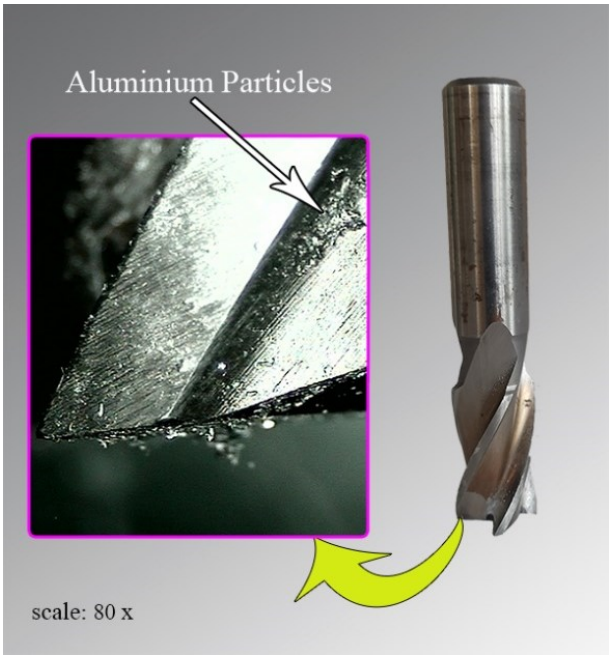

Fig. 10. Presence of piled up aluminum particles on the tool face.

resulting in a better surface finish.

It is also determined that the NECAPed process on the workpiece improves surface finish by 8.47% compared to the primary workpiece for various feed rates exerted during different spindle speeds.

3.4. Chip formation analysis

The resulting chips related to each experiment were collected, and some of them are illustrated in Fig. 11. It is observed that the shape of the chips is influenced by cutting conditions in terms of spindle speed, feed rate and depth of cut. In the subject of chip disposal, ductile materials have the potential to produce long and continuous chips. A major problem encountered in machining ductile materials is the formation of long chips. They gather around the workpiece and the surface of the newly machined workpiece and stratch them that leads to a poor surface finish. Generally, lower hardness values in materials provide long chips, while brittle materials give a better surface finish.

Considering the aforementioned issues, the short and discontinuous chip is favorable that this form is obtained by using high spindle speed and low feed rate. On the other hand, long and continuous chips are produced in low spindle speed and high feed rate condition. As is clear in Fig. 11, the obtained primary workpiece chips (Fig. 11(a)) are continuous due to their cutting conditions, while the NECAPed workpiece chips (Fig. 11(b)) produced in a similar cutting condition are fragmented, resulting in a better surface finish. It means that in a NECAPed workpiece, even the cutting condition that leads to the formation of long and continuous chips, produces short and discontinuous chips due to the brittle nature of the NECAPed workpiece.

On the other hand, in some cutting conditions (Fig. 11(c) and (d)), at first glance, the primary and NECAPed workpieces appear to produce a similar chip under the same cutting conditions, although NECAPed workpiece chips have a relatively smaller curvature. It must be pointed out that scanning electron microscope (SEM) images (× 1000 magnification) of both workpiece chips reveal the significant characteristic of the chips produced. As shown in Fig. 12, at a small feed rate, numerous cracks were observed on the NECAPed workpiece chips, which are evidence of brittle fracture. Small and curled chips are obtained at high spindle speed, perhaps due to the thermal softening of the workpiece.

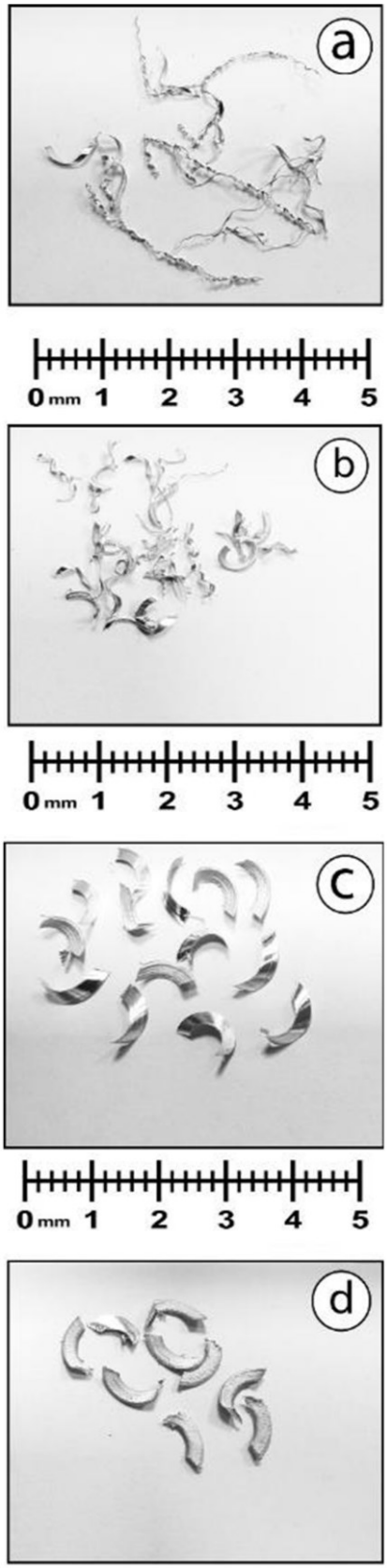

Fig. 11. Chip formation of (a) primary workpiece chips (n=565 rev/min, f=200 mm/min, a_p=1.5 mm), (b) NECAPed workpiece chips (n=565 rev/min, f=200 mm/min, a_p=1.5 mm), (c) primary workpiece chips (n=1500 rev/min, f=98 mm/min, a_p=0.5 mm), (d) NECAPed workpiece chips (n=1500 rev/min, f=98 mm/min, a_p=0.5 mm).

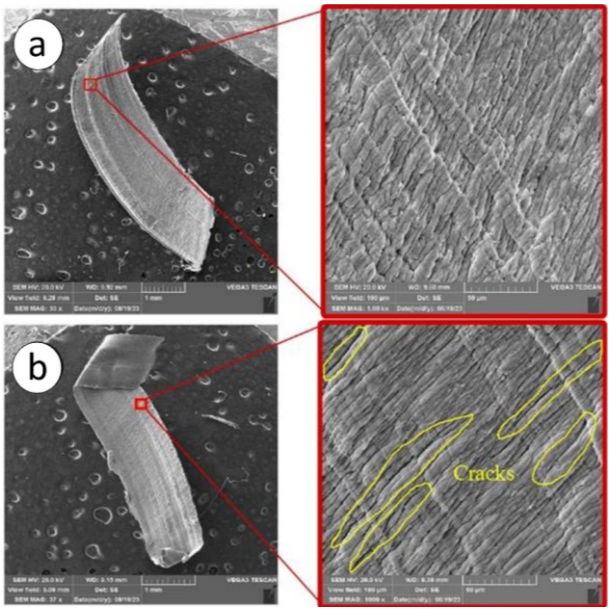

Fig. 12. SEM of (a) primary and (b) NECAPed workpieces (n=1500 rev/min, f=98 mm/min, a_p=0.5 mm).

4. Conclusions

In this article, the influence of non-equal-channel angular pressing (NECAP) on the machinability of Al 3003 was explored. The investigation focuses on the effects of milling operation input variables, namely spindle speed, feed rate, and depth of cut, on cutting force, surface roughness, and chip morphology as output results. Implementation of SPD in the NECAP form improves determined machinability aspects of Al 3003, in which cutting force and surface roughness are reduced and chip formation is enhanced. According to a machining analysis, several significant remarks are concluded:

- Significant promotion of NECAPed workpiece material properties in terms of lower ductility and higher hardness and UTS, due to the NECAP implementation, is a fundamental factor to achieve better machinability.
- The minimum cutting force was determined at lower spindle speed and depth of cut for primary and NECAPed workpiece. The smaller the feed rate, the lower the cutting force. When the spindle speed is increased during machining, the cutting forces decrease because of heat generation that leads to the softening effect, resulting in low

frictional forces acting on the tool.

- The smaller the feed rate and depth of cut, the better the surface finish for both workpieces. The NECAPed workpiece diminished material adhesion helps prevent BUL formation, leading to a superior surface finish and lower cutting force.
- Due to the brittle properties of the NECAPed workpiece in comparison to the primary workpiece, when exposed to similar cutting conditions, its produced chips are likely to break more readily, improving finishing.

Conflict of interest

The authors declare no competing interests.

Funding

The authors declare that no funds were received during the preparation of this manuscript.

5. References

[1] Radhi, H. N., Aljassani, A. M., & Mohammed, M. T. (2020). Effect of ECAP on microstructure, mechanical and tribological properties of aluminum and brass alloys: A review. *Materials Today: Proceedings*, *26*, 2302-2307. https://doi.org/10.1016/j.matpr.2020.02.497

[2] Ramesh Kumar, S., Gudimetla, K., Mohanlal, S., & Ravisankar, B. (2019). Effect of mechanically alloyed graphene-reinforced aluminium by equal channel angular pressing (ECAP). *Transactions of the Indian Institute of Metals*, *72*(6), 1437-1441. https://doi.org/10.1007/s12666-019-01715-y

[3] Bagherpour, E., Reihanian, M., Pardis, M., Ebrahimi, R., & Langdon, T. G. (2018). Ten years of severe plastic deformation (SPD) in Iran, part I: Equal-channel angular pressing (ECAP). *Iranian Journal of Materials Forming*, *5*(1), 71–113. http://dx.doi.org/10.22099/IJMF.2018.28756.1101

[4] Bagherpour, E., Pardis, N., Reihanian, M., & Ebrahimi, R. (2019). An overview on severe plastic deformation: research status, techniques classification, microstructure evolution, and applications. *The International Journal of Advanced Manufacturing Technology*, *100*, 1647-1694. https://doi.org/10.1007/s00170-018-2652-z

[5] Azushima, A., Kopp, R., Korhonen, A., Yang, D. Y., Micari, F., Lahoti, G. D., Groche, P., Yanagimoto, J., Tsuji, N., Rosochowski, A., & Yanagida, A. (2008). Severe plastic deformation (SPD) processes for metals. *CIRP annals*, *57*(2), 716-735. https://doi.org/10.1016/j.cirp.2008.09.005

[6] Segal, V. (2018). Review: Modes and processes of severe plastic deformation (SPD). *Materials*, *11*(7), 1175. https://doi.org/10.3390/ma11071175

[7] Khodabakhshi, F., Mohammadi, M., & Gerlich, A. P. (2021). Stability of ultra-fine and nano-grains after severe plastic deformation: A critical review. *Journal of Materials Science*, *56*(28), 15513-15537. https://doi.org/10.1007/s10853-021-06274-6

[8] Gupta, A., Saxena, K. K., Bharti, A., Lade, J., Chadha, K., & Paresi, P. R. (2022). Influence of ECAP processing temperature and number of passes on hardness and microstructure of Al-6063. *Advances in Materials and Processing Technologies*, *8*, 1635-1646. https://doi.org/10.1080/2374068X.2021.1953917

[9] Saxena, K. K., Kumar, K. B., & Gupta, A. (2021). Effect of processing parameters on equal-channel angular pressing of aluminum alloys: an overview. *Materials Today: Proceedings*, *45*, 5551-5559. https://doi.org/10.1016/j.matpr.2021.02.303

[10] Hasani, A., Tóth, L. S., & Beausir, B. (2010). Principles of nonequal channel angular pressing. *Journal of Engineering Materials and Technology*, *132*(3), 0310011–0310019. https://doi.org/10.1115/1.4001261

[11] Gu, C. F., & Toth, L. S. (2012). Texture development and grain refinement in non-equal-channel angular-pressed Al. *Scripta Materialia*, *67*(1), 33-36. https://doi.org/10.1016/j.scriptamat.2012.03.014

[12] Fereshteh-Saniee, F., Asgari, M., & Fakhar, N. (2016). Specialized mechanical properties of pure aluminum by using non-equal channel angular pressing for developing its electrical applications. *Applied Physics A: Materials Science and Processing*, *122*(8), 1-12. https://doi.org/10.1007/s00339-016-0305-3

[13] Asgari, M., Fereshteh-Saniee, F., Pezeshki, S. M., & Barati, M. (2016). Non-equal channel angular pressing (NECAP) of AZ80 Magnesium alloy: Effects of process parameters on strain homogeneity, grain refinement and mechanical properties. *Materials Science and Engineering: A*, *678*, 320-328. https://doi.org/10.1016/j.msea.2016.09.102

[14] Asgari, M., & Fereshteh-Saniee, F. (2016). Production of AZ80/Al composite rods employing non-equal channel lateral extrusion. *Transactions of Nonferrous Metals Society of China*, *26*(5), 1276-1283. https://doi.org/10.1016/S1003-6326(16)64228-0

[15] Tóth, L. S., Lapovok, R., Hasani, A., & Gu, C. (2009). Non-equal channel angular pressing of aluminum alloy. *Scripta Materialia*, *61*(12), 1121-1124. https://doi.org/10.1016/j.scriptamat.2009.09.006

[16] Khanlari, H., & Honarpisheh, M. (2020). Investigation of microstructure, mechanical properties and residual stress in non-equal-channel angular pressing of 6061 aluminum alloy. *Transactions of the Indian Institute of Metals*, *73*(5), 1109-1121. https://doi.org/10.1007/s12666-020-01945-5

[17] Fereshteh-Saniee, F., Asgari, M., Barati, M., & Pezeshki, S. M. (2014). Effects of die geometry on non-equal channel lateral extru sion (NECLE) of AZ80 magnesium alloy. *Transactions of Nonferrous Metals Society of China*, *24*(10), 3274-3284. https://doi.org/10.1016/S1003-6326(14)63467-1

[18] Khanlari, H., & Honarpisheh, M. (2023). An upper bound analysis of channel angular pressing process considering die geometric characteristics, friction, and material strain-hardening. *CIRP Journal of Manufacturing Science and Technology*, *41*, 259-276. https://doi.org/10.1016/j.cirpj.2022.12.007

[19] Rajeswari, B., & Amirthagadeswaran, K. S. (2018). Study of machinability and parametric optimization of end milling on aluminium hybrid composites using multi-objective genetic algorithm. *Journal of the Brazilian Society of Mechanical Sciences and Engineering*, *40*(8), 1-15. https://doi.org/10.1007/s40430-018-1293-3

[20] Pradhan, S., Indraneel, S., Sharma, R., Bagal, D. K., & Bathe, R. N. (2020). Optimization of machinability criteria during dry machining of Ti-2 with micro-groove cutting tool using WASPAS approach. *Materials Today: Proceedings*, *33*, 5306-5312. https://doi.org/10.1016/j.matpr.2020.02.972

[21] Kanaujia, N., Rahul, Behera, J. K., Mohapatra, S. K., Behera, A., Jha, P., Joshi, K. K., & Routara, B. C. (2022). Process parameters optimization in CNC turning of aluminum 7075 alloy using TOPSIS method coupled with Taguchi philosophy. *Materials Today: Proceedings*, *56*, 989-994. https://doi.org/10.1016/j.matpr.2022.03.226

[22] Wagri, N. K., Petare, A., Agrawal, A., Rai, R., Malviya, R., Dohare, S., & Kishore, K. (2022). An overview of the machinability of alloy steel. *Materials Today: Proceedings*, *62*, 3771-3781. https://doi.org/10.1016/j.matpr.2022.04.457

[23] Zhao, Z., To, S., Wang, J., Zhang, G., & Weng, Z. (2022). A review of micro/nanostructure effects on the machining of metallic materials. *Materials & Design*, *224*, 111315. https://doi.org/10.1016/j.matdes.2022.111315

[24] Sinha, M. K., Pal, A., Kishore, K., Singh, A., Archana, Sansanwal, H., & Sharma, P. (2023). Applications of sustainable techniques in machinability improvement of superalloys: a comprehensive review. *International Journal on Interactive Design and Manufacturing (IJIDeM)*, *17*(2), 473-498. https://doi.org/10.1007/s12008-022-01053-2

[25] Paturi, U. M. R., & Reddy, N. S. (2021). Progress of machinability on the machining of Inconel 718: A comprehensive review on the perception of cleaner machining. *Cleaner Engineering and Technology*, *5*, 100323. https://doi.org/10.1016/j.clet.2021.100323

[26] Kar, S., & Patowari, P. K. (2019). Experimental investigation of machinability and surface characteristics in microelectrical discharge milling of titanium, stainless steel and copper. *Arabian Journal for Science and Engineering*, *44*(9), 7843-7858. https://doi.org/10.1007/s13369-019-03918-3

[27] Santos, M. C., Machado, A. R., Sales, W. F., Barrozo, M. A., & Ezugwu, E. O. (2016). Machining of aluminum alloys: a review. *The International Journal of Advanced Manufacturing Technology*, *86*, 3067-3080. https://doi.org/10.1007/s00170-016-8431-9

[28] Soren, T. R., Kumar, R., Panigrahi, I., Sahoo, A. K., Panda, A., & Das, R. K. (2019). Machinability behavior of aluminium alloys: A brief study. *Materials Today: Proceedings*, *18*, 5069-5075. https://doi.org/10.1016/j.matpr.2019.07.502

[29] Sukumar, M. S., Ramaiah, P. V., & Nagarjuna, A. (2014). Optimization and prediction of parameters in face milling of Al-6061 using Taguchi and ANN approach. *Procedia Engineering*, *97*, 365-371. https://doi.org/10.1016/j.proeng.2014.12.260

[30] Pan, J., Ni, J., He, L., Cui, Z., & Feng, K. (2020). Influence of micro-structured milling cutter on the milling load and surface roughness of 6061 aluminum alloy. *The International Journal of Advanced Manufacturing Technology*, *110*, 3201-3208. https://doi.org/10.1007/s00170-020-06080-5

[31] Mahanta, T. K., Lam, R. R., Chakrapani, Y., Irulappasamy, S., Dumpala, R., & Sunil, B. R. (2022). Machining characteristics of Al6063 composites reinforced with SiC particles. *Materials Today: Proceedings*, *50*, 2351-2354. https://doi.org/10.1016/j.matpr.2021.10.235

[32] Sreejith, P. S. (2008). Machining of 6061 aluminium alloy with MQL, dry and flooded lubricant conditions. *Materials letters*, *62*(2), 276-278. https://doi.org/10.1016/j.matlet.2007.05.019

[33] Rahmati, B., Sarhan, A. A., & Sayuti, M. (2014). Morphology of surface generated by end milling AL6061-T6 using molybdenum disulfide (MoS_2) nanolubrication in end milling machining. *Journal of Cleaner Production*, *66*, 685-691. https://doi.org/10.1016/j.jclepro.2013.10.048

[34] Deswal, N., & Kant, R. (2022). Machinability analysis during laser assisted turning of aluminium 3003 alloy. *Lasers in Manufacturing and Materials*

Processing, *9*(1), 56-71. https://doi.org/10.1007/s40516-022-00163-9

[35] Yang, J., Zhang, Y., Huang, Y., Lv, J., & Wang, K. (2023). Multi-objective optimization of milling process: exploring trade-off among energy consumption, time consumption and surface roughness. *International Journal of Computer Integrated Manufacturing*, *36*(2), 219-238. https://doi.org/10.1080/0951192X.2022.2078511

[36] Wiesinger, G., Baumann, C., & Krystian, M. (2018). Impact of Equal Channel Angular Pressing (ECAP) on the machinability of an aluminium alloy (EN AW-6082). *Materials Today: Proceedings*, *5*(13), 26654-26660. https://doi.org/10.1016/j.matpr.2018.08.131

[37] Iyappan, S. K., Karthikeyan, S., Ravikumar, K., Makkar, S., Rutvi Uday, K., & R. V, M. (2022). Mechanical properties and machinability of aluminium and aluminium-silicon carbide composites processed by Equal Channel Angular Pressing (ECAP). *Advances in Materials and Processing Technologies*, *8*(1), 783-796. https://doi.org/10.1080/2374068X.2020.1833402

[38] Fatahi Dolatabadi, J., Rafiee, M. M., Hadad, M., Faraji, G., & Hedayati-dezfooli, M. (2022). Experimental investigation of the effects of cutting parameters on machinability of ECAP-processed ultrafine-grained copper using tungsten carbide cutting tools. *Energy Equipment and Systems*, *10*(3), 241-254. 10.22059/EES.2022.254725

[39] Skiba, J., Kossakowska, J., Kulczyk, M., Pachla, W., Przybysz, S., Smalc-Koziorowska, J., & Przybysz, M. (2020). The impact of severe plastic deformations obtained by hydrostatic extrusion on the machinability of ultrafine-grained AA5083 alloy. *Journal of Manufacturing Processes*, *58*, 1232-1240. https://doi.org/10.1016/j.jmapro.2020.09.023

[40] Bandapalli, C., Singh, K. K., Sutaria, B. M., & Bhatt, D. V. (2016). Experimental investigation of machinability parameters in high-speed micro-end milling of titanium (grade-2). *The International Journal of Advanced Manufacturing Technology*, *85*, 2139-2153. https://doi.org/10.1007/s00170-015-7443-1

[41] Pathak, B. N., Sahoo, K. L., & Mishra, M. (2013). Effect of machining parameters on cutting forces and surface roughness in Al-(1-2) Fe-1V-1Si alloys. *Materials and Manufacturing Processes*, *28*(4), 463-469. https://doi.org/10.1080/10426914.2013.763952